EPS95 Ref. **eps 0518**
Submitted to **Pa–10, Pa–17**
Pl–01, Pl–02

EUROPEAN ORGANIZATION FOR NUCLEAR RESEARCH

A Study of the String Effect in $Z \rightarrow 3$ Jets

The ALEPH Collaboration

Abstract

The string effect is analyzed in events of the type $Z \rightarrow q\overline{q}$ with a hard gluon radiated. This effect is caused by color forces between the gluon and the two quarks in $q\overline{q}g$-events, leading to increased final state particle densities between a gluon and a quark. Three–jet events are selected by applying a cluster algorithm to the charged and neutral particles measured with the ALEPH detector at the LEP collider. Exploiting the fact that, in QCD, jet 3 is the gluon jet with high probability if the jets are numbered according to their energy ($E_1 > E_2 > E_3$), two observables sensitive to the string effect are studied: the ratio $\mathcal{R} := N_{1,3}/N_{1,2}$ of inter-jet particle flow, with and without momentum weighting, and $\Delta\phi$, the angular shift between the leading particle and the total jet vector for jets 1 and 2. Using these observables the string effect is clearly seen in the data. Comparing the experimental results with predictions from various QCD Monte Carlo models, perturbative effects as well as different mechanisms in the hadronization process are identified, which are contributing to the string effect.

Contribution to the International Europhysics Conference on High Energy Physics, Brussels, Belgium, 27 July – 2 August 1995

1 Introduction

The radiation of a hard non-collinear gluon from one of the quarks in the annihilation process $e^+e^- \to q\overline{q}$ at high energy leads to events with three well-separated hadronic jets. The azimuthal distribution of particles in the event plane has been shown to be a sensitive probe of hadron production models. The term "string effect" denotes the experimental observation of enhanced particle flow into the angular region between quark and gluon jet as compared to quark and antiquark jet. The effect, first seen by the JADE collaboration [1, 2] and later confirmed by other PETRA/PEP experiments [3, 4], was found to be better reproduced by the color string model of the Lund group than by independent jet fragmentation. It has further been shown that soft gluon interference plays an important role [5]. In these types of analyses it is essential to tag the gluon jet. This was achieved by energy ordering: according to perturbative QCD the lowest energy jet is the gluon jet with a high probability depending on the kinematic configuration. Using heavy quark jet tagging, the OPAL collaboration at LEP was able to confirm the existence of the string effect in the data in a model independent way [6].

In the present work it is shown that not only the inter-jet particle flow is sensitive to the string effect, but also the particle distribution within the quark jets. The variables used are the standard ratios $\mathcal{R}$ ($\mathcal{R}_p$) of inter-jet particle (momentum) flow and the angle shift $\Delta\phi(\mathbf{L1})$ between the leading particle and total jet vector of the highest and second highest energy jets. The latter variable is sensitive to the momentum dependence of particle directions within a jet. Energy ordering is used to tag the gluon jet which allows to use the full data statistics. The results are compared to a variety of QCD + hadronisation models [10, 11, 12, 13].

2 Event selection and 3-jet kinematics

Hadronic events were required to have at least 5 good charged tracks summing up to at least 10 % of the center-of-mass energy, E_{cm}. This selects 728 000 (690 000) events from the 1992 (1993) data taking period at $E_{cm} = m_Z$. The 1993 data include the sideband energies $m_Z \pm 2$ GeV. A sample of 1.8×10^6 fully simulated Jetset 7.3 Monte Carlo events was used to perform the detector corrections. The particles in an event are reconstructed by an energy flow algorithm (described in detail in [7]) which uses information from most of the Aleph subdetectors: charged tracks from the tracking system and neutral clusters from the electromagnetic and hadronic calorimeters, called E–flow objects in the following. Further cuts on the event sample are slightly different for the two analyses: for the $\mathcal{R}$–analysis at least 15 E–flow objects are required summing up to an energy of at least 30 GeV, while for the $\Delta\phi$ analysis the energy sum of the E–flow objects is required to exceed $E_{cm}/2$ and the angle of the thrust axis with respect to the beam direction has to exceed 30°.

The jets in each event are defined through a cluster algorithm of the Durham (or $k_\perp$) type [8] based on the metric

$$y_{ik} := \frac{2\min(E_i^2, E_k^2)(1-\cos\Theta_{ik})}{E_{vis}^2} \; .$$

The two E–flow particles with the smallest y_{ik} are replaced by a pseudo–particle with 4–momentum $p = p_i + p_k$. This procedure is repeated as long as the smallest y_{ik} does not exceed a preselected cut-off value y_{cut}. The clusters found at the final stage are called jets. At a typical value $y_{cut} = 0.01$ the 3-jet production rate (corrected for detector effects) is measured to be 0.304 ± 0.003, and the 4-jet rate is still relatively small (0.051 ± 0.001). While the predictions of the QCD generators Herwig and ARIADNE for the 3-jet rate (0.305 and 0.306) agree well with the data, the corresponding JETSET number (0.327) is significantly higher. The excess is found to be concentrated in kinematic region **R1**, defined in figure 1.

Three–jet events are selected for the further analysis. From the 3 jet vectors an average event plane is constructed and all jet and particle momenta are projected into this plane. For the $\mathcal{R}$–analysis the polar angle between the normal vector to the event plane and the beam direction is required to be less than 60° in order to ensure good particle acceptance also in the interjet regions. For the $\Delta\phi$ analysis the polar angle of each jet is instead required to be larger than 30°. Events were excluded if a single photon carries > 85 % of the energy of one of the three jets ($q\bar{q}\gamma$ events). Utilizing the good angular resolution of ALEPH and energy–momentum conservation the jet energies are reconstructed using the jet–jet angles:

$$E_{i,rec} = \frac{\sin\Phi_{j,k}}{\sin\Phi_{1,2} + \sin\Phi_{1,3} + \sin\Phi_{2,3}}\, E_{cm}$$

with i,j,k cyclic, giving a much better energy resolution (between 1 and 2 GeV) than using the measured jet energies directly. The jets are ordered such that $x_1 > x_2 > x_3$, where $x_i = 2E_{i,rec}/E_{cm}$ are the scaled jet energies and $x_1 + x_2 + x_3 = 2$. The same procedure is also applied to the Monte Carlo calculations. The population density of ALEPH data with respect to two independent variables chosen as

$$\mathcal{Z} = \frac{(x_2 - x_3)}{\sqrt{3}} \qquad \text{and} \qquad \Phi_{1,3}$$

is shown in figure 1 for a central value of y_{cut}. The motivation for choosing these variables is that

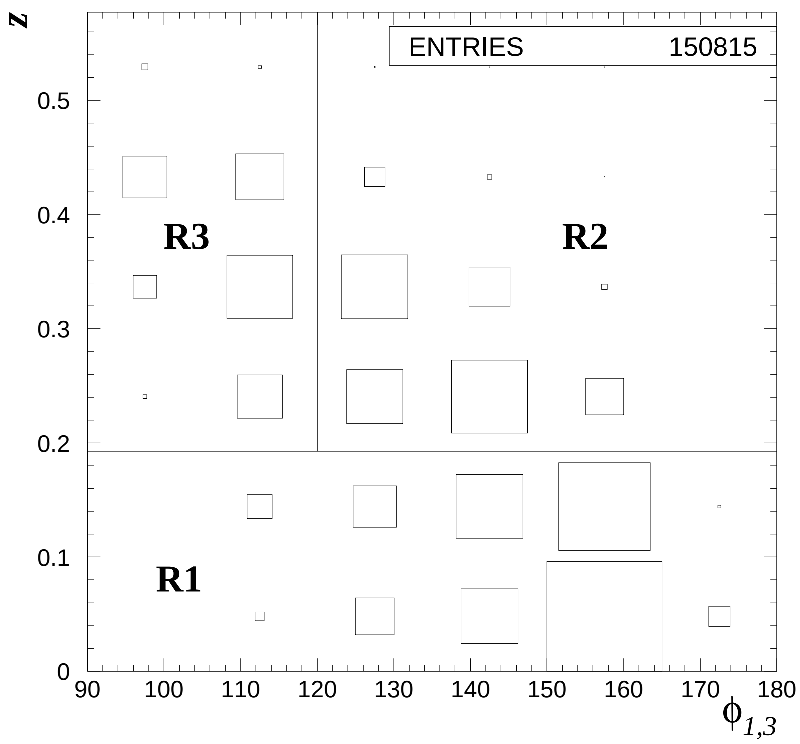

Figure 1: Distribution of 3–jet events in the 2-dimensional $\mathcal{Z}$ versus $\Phi_{1,3}$ plot for the central $y_{cut} = 0.01$. The size of the boxes corresponds to the population density for the ALEPH 1992 data sample. Kinematic regions characterized by different event properties are indicated by **R1**, **R2** and **R3**.

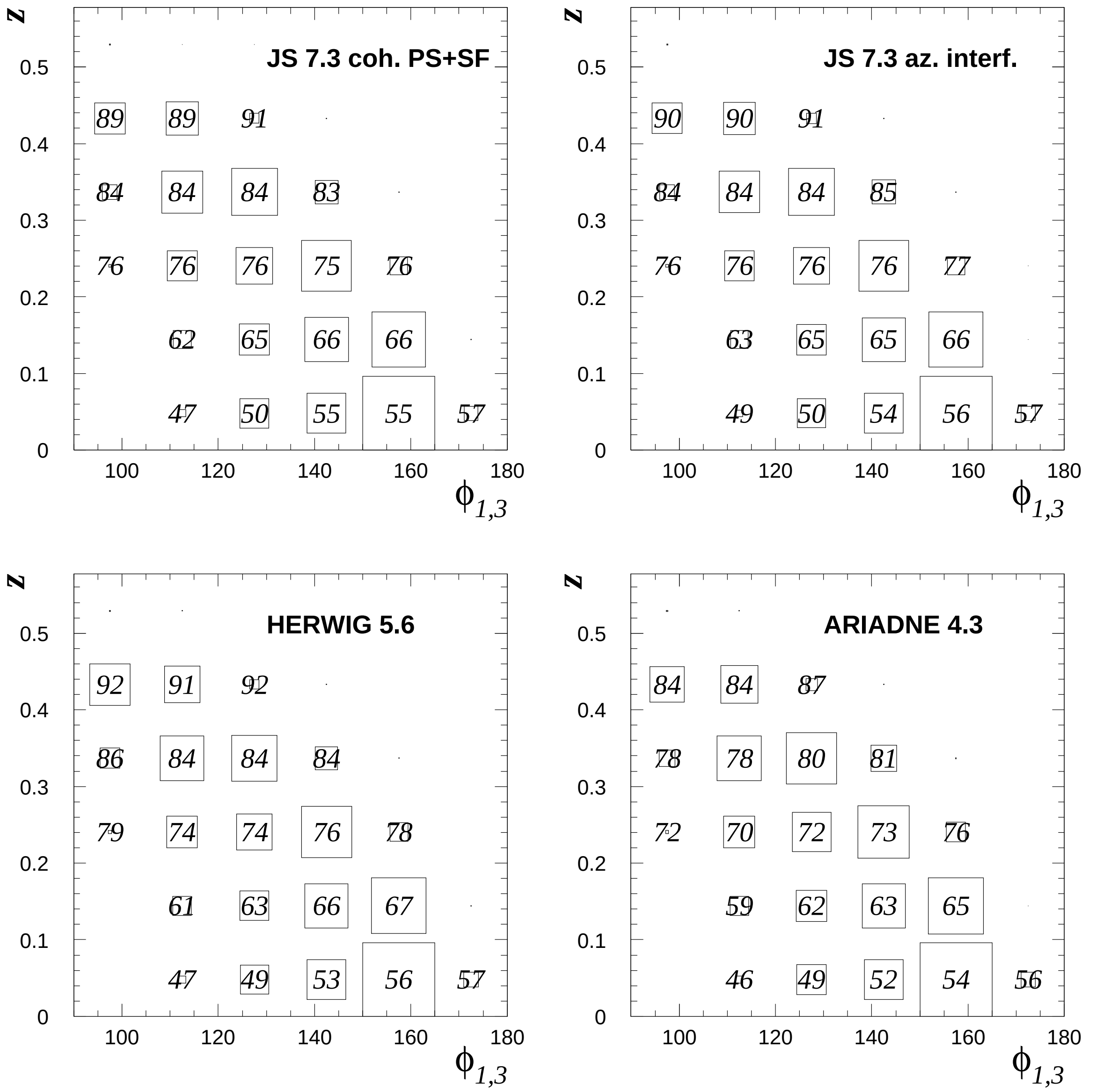

Figure 2: Probability $P_{3=\mathrm{g}}$ (in %) for the 3-rd jet to be the gluon jet for some standard QCD Monte Carlo models, for $y_{cut} = 0.01$ (no detector simulation). The boxes indicate the population densities at hadron level.

the strength of the string effect is expected to depend both on the quark–gluon opening angle and on the energy difference $\mathcal{Z}$. The latter dependence is related to the probability $P_{3=\mathrm{g}}$ for jet 3 being the gluon jet, which for regions **R2** and **R3** depends mainly on $\mathcal{Z}$. This is demonstrated in figure 2 which shows QCD model calculations of $P_{3=\mathrm{g}}$. The gluon jet is defined as the hadron level jet which is matched in angle to the parton level gluon jet. The latter is defined at the end of the parton shower as the jet which has an equal number of quarks and antiquarks (no net baryon number). The numbers for $P_{3=\mathrm{g}}$ are very similar for Jetset and Herwig and slightly lower for Ariadne. They are expected to be similar since the calculations are all based on perturbative QCD. The probability for the highest energy jet to be a quark jet, $P_{1=\mathrm{q}}$, is always above 90%.

Monte Carlo studies show that the observable size of the string effect increases with increasing $\mathcal{Z}$ or decreasing $\Phi_{1,3}$. This motivates the definition of the 3 regions in 3–jet phase space as indicated in figure 1, with boundaries at $\mathcal{Z} = 1/(3\sqrt{3})$ and $\Phi_{1,3} = 120°$. The analyses are carried out in the full 3–jet phase space but also in the 3 regions separately. In **R3**, which turns out to be the most sensitive region, jet 3 has rather low energy ($\langle x_3 \rangle = 0.236$) but is well separated in angle from the two high energy jets having $x_1 = 0.904$ and $x_2 = 0.860$ on average. Here the JETSET results for the probabilities $P_{3=\mathrm{g}}$ and $P_{1=\mathrm{q}}$ are 84 % and 94 %, respectively.

3 Interjet particle flow

Figure 3 illustrates the definition of the interjet regions. Each 3–jet event is oriented such that

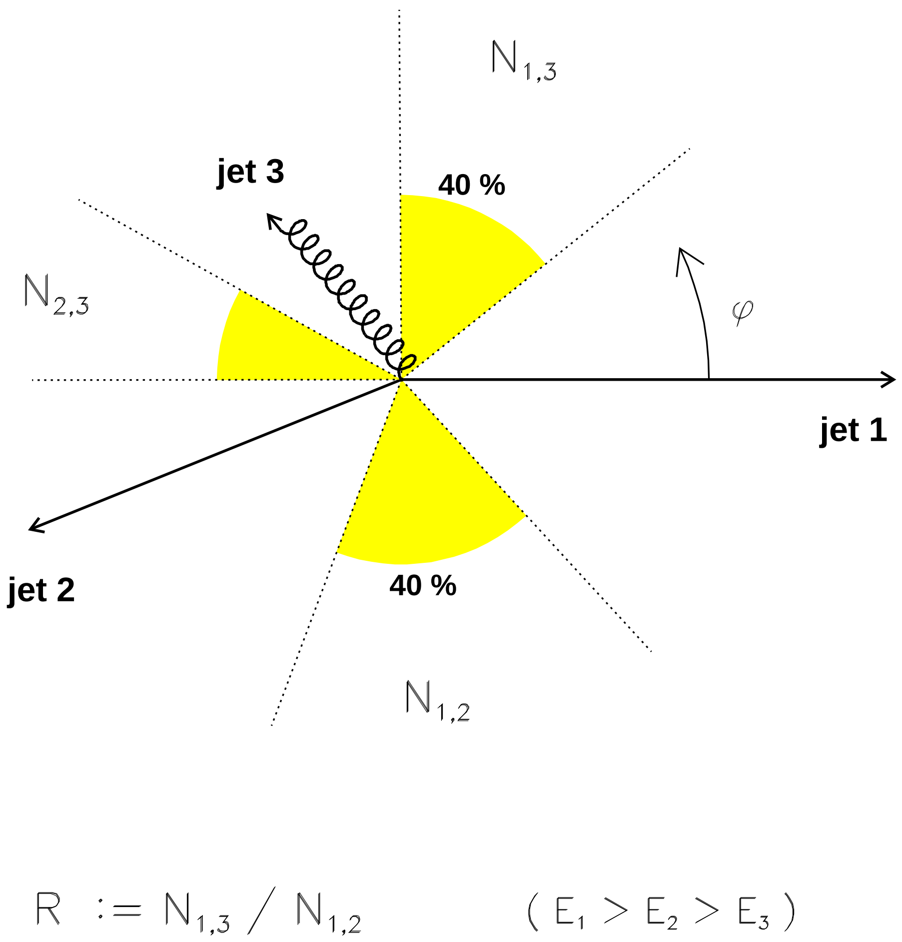

Figure 3: Definition of the ratio $\mathcal{R}$ which measures the strength of the string effect.

jet 1 is at $\Phi = 0$ and jet 3 has $\Phi > 0$. In order to compensate the event-to-event variation of the jet directions it is convenient to consider the reduced particle angle

$$\varphi' = \frac{\varphi - \Phi_i}{\Phi_k - \Phi_i} ,$$

where the particle under consideration is located between jets i and k ($\Phi_i < \varphi < \Phi_k$). The particle distribution as function of φ' is shown in figure 4 for the 1992 data sample, normalized to the 112 000 three–jet events selected with the cuts described above at a central value of $y_{cut} = 0.009$.

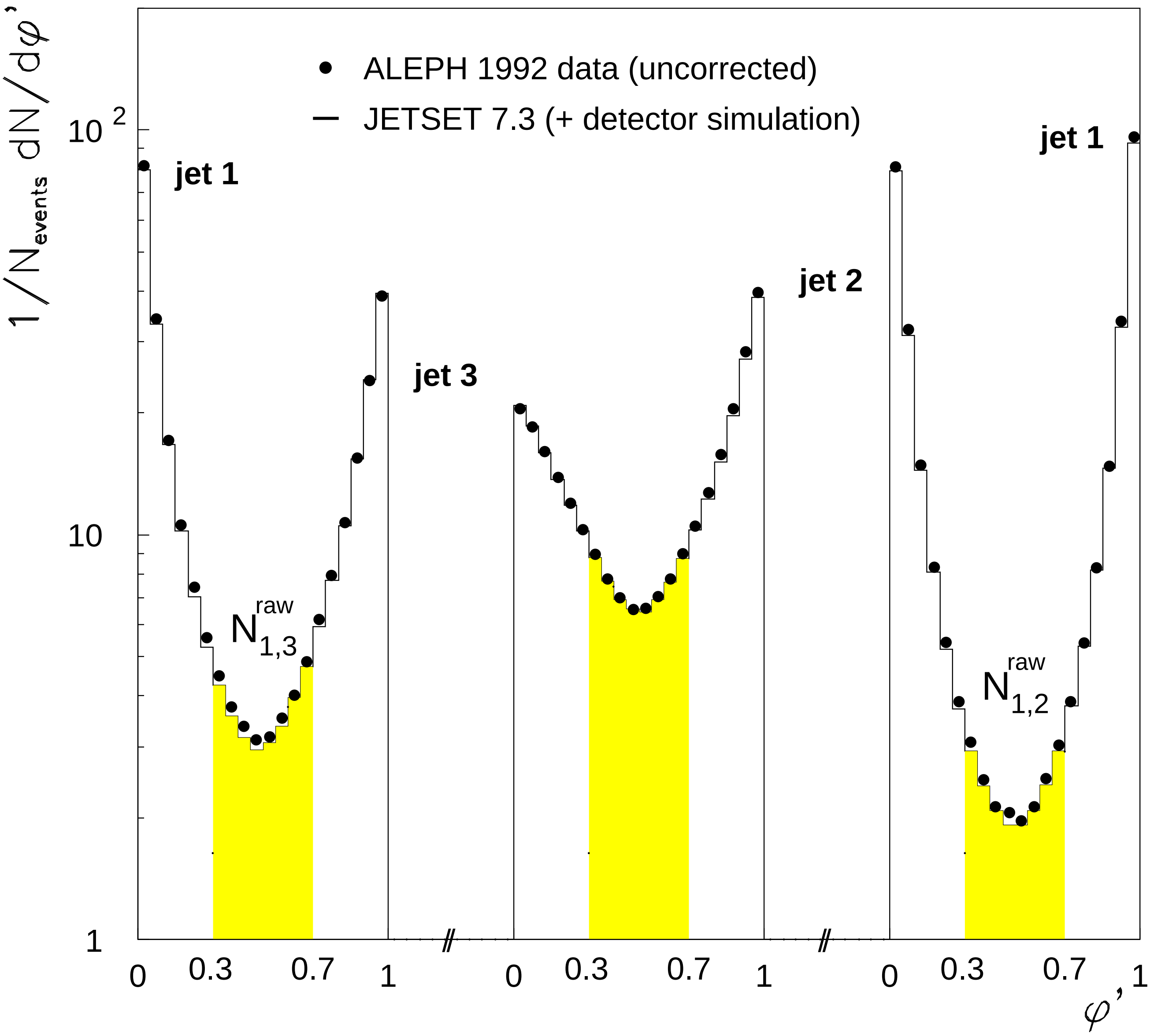

Figure 4: Particle density (normalized to the number of 3–jet events) between jet axes in 3-jet events as a function of the reduced angle φ'. The shaded parts of the distributions correspond to the particles used in the analysis.

The JETSET model is seen to describe the data rather well. The interjet regions, defined as the central 40 % of the angular regions ($0.3 < \varphi' < 0.7$) are marked as shaded areas in figures 3 and 4. The average momentum of particles in these regions is between 0.6 and 0.7 GeV/c.

The ratio of particle yield and the ratio of momentum flow measured for the whole 3-jet phase space are

$$\mathcal{R} = \frac{N_{1,3}}{N_{1,2}} = 1.384 \pm 0.007\,(stat) \pm 0.035\,(syst)$$

$$\mathcal{R}_p = \frac{(\sum |p|)_{1,3}}{(\sum |p|)_{1,2}} = 1.731 \pm 0.012\,(stat) \pm 0.029\,(syst)\ .$$

Before computing these numbers the φ' distributions were corrected for detector effects using bin-by-bin correction factors. The systematic error estimates quoted are the result of three contributions which have been added in quadrature: (1) variation of the track cuts, (2) variation of the event cuts and (3) using different event generators to perform the corrections. In this case a simplified detector simulation was used.

The measured numbers are clearly larger than 1 indicating an enhanced particle production in the angular region between the quark and the gluon jet. In addition, the effect increases with momentum, as seen from the fact that $\mathcal{R}_p > \mathcal{R}$. A quantitative interpretation can be obtained from a comparison to QCD model calculations.

Figure 5 shows the data together with predictions of several standard QCD generators and of a number of JETSET variants. A breakdown of the string effect into perturbative and non–perturbative contributions is given in figure 6. The most important free parameters of these generators (except COJETS) have been tuned to best describe global event shape and inclusive charged particle spectra [9]. It should be stressed that the data presented in sections 3 and 4 have *not* been included in the tuning, *i.e.* the Monte Carlo calculations are *predictions* of the string effect in the context of globally tuned models.

The prediction of the JETSET version 7.3 coherent parton shower + string fragmentation model [10] (uppermost points in figure 5) is in excellent agreement with the data although the prediction depends slightly on the parameter tuning. *2-nd tuning* means that the multi–parameter fit was performed to a more recent data set, the main difference being a lower value for the shower cut-off: $Q_0 = 1.57 \rightarrow 1.21$ GeV. It is seen from figure 6 that the string effect is already present at the parton level, but gets additional contributions from the string hadronization. The effect on hadron level is slightly reduced if the perturbative phase extends further down to lower masses (*2-nd tuning*).

Looking at variants of JETSET one finds that the $\mathcal{R}$ values decrease and are no longer in good agreement with the data if the angular ordering in the shower development is switched off (*incoherent*). On parton level the effect is even more pronounced, demonstrating that soft gluon interference does create a string effect already in the perturbative phase. Another source of the string effect on parton level are azimuthal correlations. The $\mathcal{R}$ values increase if azimuthal anisotropy in gluon decay due to interference is included (*azimuthal interference*), in addition to angular ordering.

The hypothesis of color strings between all 3 hard partons in a 3-jet event can be probed with the *closed string* model. This variant is a toy model in which the shower is assumed to start from a gluon–gluon state instead of a $q\overline{q}$ state. In order to obtain reasonable particle multiplicities a very low QCD scale $\Lambda \approx 1$ MeV has to be inserted. Since a gluon carries two color indices the string configuration is that of a closed string (in the absence of extra $q\overline{q}$ pairs). This model gives a too low effect and is thus clearly excluded by the data.

The smallest $\mathcal{R}$ values (close to 1) are obtained in the case of the JETSET $\mathcal{O}(\alpha_S^2)$ matrix element generator combined with independent fragmentation, which is clearly rejected by the data. Using string fragmentation instead, gives results very similar to the parton shower model, even though the matrix element model does not reproduce other features of hadronic events, like the momentum spectrum [9]. In the context of matrix element models the string effect can be interpreted as being due to non-perturbative effects only. The fact that coherent parton shower models exhibit the string effect already in the perturbative phase thus demonstrates that the Lund string is able to parametrize some features of perturbative QCD.

The predictions of the HERWIG generator [11] which is also based on a coherent parton shower but uses a cluster hadronization model, are only slightly lower than those of JETSET. This

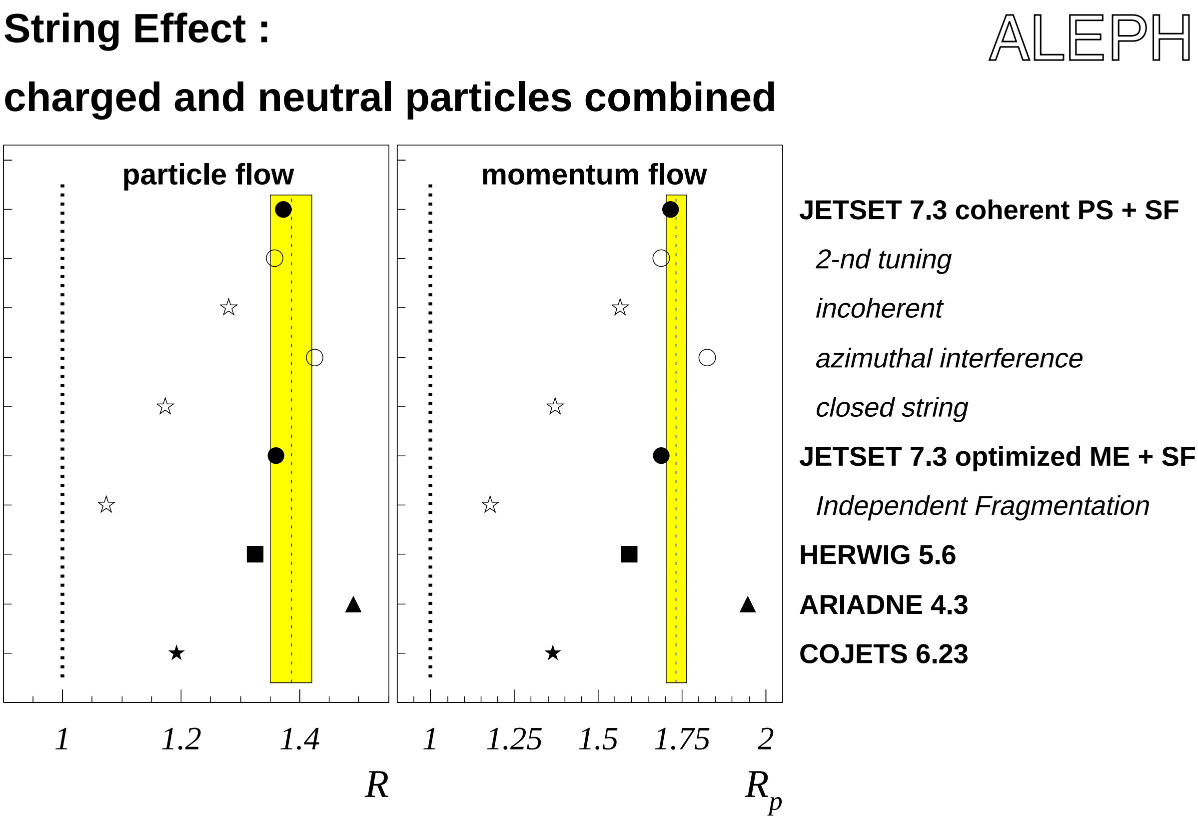

Figure 5: Values of inter-jet particle flow and momentum flow ratios of corrected data (the shaded bands indicate the total error) and various QCD models.

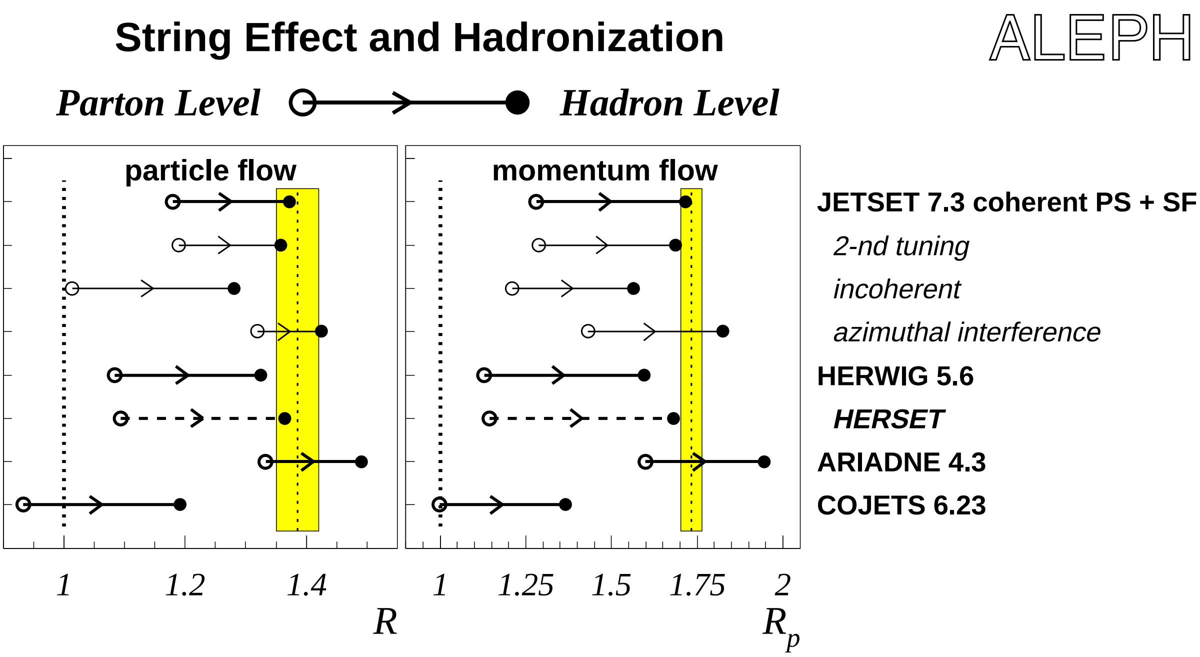

Figure 6: The same as figure 5, but the QCD model calculations at the quark-gluon level are shown in addition.

is surprising since the clusters are assumed to decay isotropically and thus have no string-like features. It seems that the HERWIG cluster model contributes a similar amount to $\mathcal{R}$ as the JETSET string model. This fact is confirmed by attaching the string model to the HERWIG parton shower ("HERSET"), and suggests that the color ordering given by the parton shower is the mechanism for producing the string effect.

The ARIADNE [12] generator which includes a color dipole formulation of the parton shower and the Lund string fragmentation model, gives distinctly higher $\mathcal{R}$ and $\mathcal{R}_p$ values, which can be traced to the high values already present at the partonic level.

A recent version of COJETS [13] which combines an incoherent parton shower with independent fragmentation gives much too low $\mathcal{R}$ values. Consistent with the JETSET incoherent parton shower, also here the string effect is absent on parton level. It should be noted that COJETS uses a much higher mass cut-off (3 GeV) than the other parton shower generators. It seems that the special treatment of large angle particle emission in COJETS also is able to produce a sizeable fragmentation contribution.

Topology dependence

The above results are obtained for the full three-jet phase space. Figure 7 shows the results separately for the three kinematic regions defined in 1. As expected from the considerations in section 2, the $\mathcal{R}$ value and the sensitivity to QCD models are largest in region **R3**.

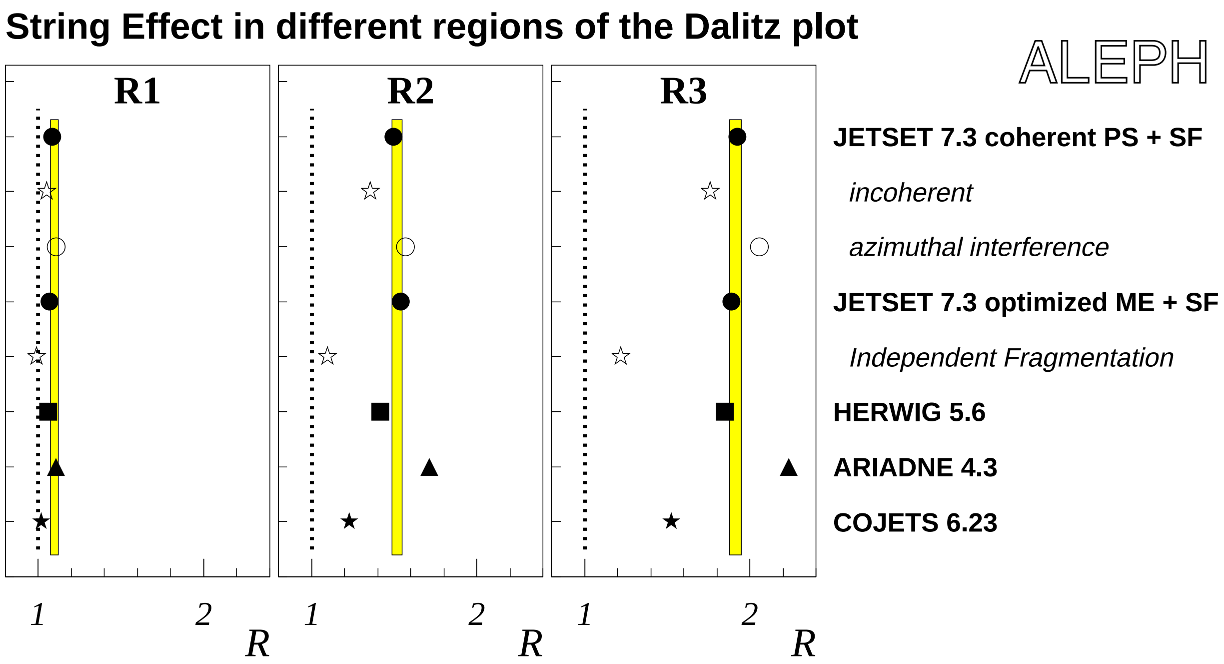

Figure 7: The inter-jet particle flow ratio of corrected data (shaded bands) and QCD models, separately in the three kinematic regions as defined in figure 1.

Dependence on the particle type

At low momentum, charged hadrons ($\pi^{\pm}, \mathrm{K}^{\pm}$ and $\overline{\mathrm{p}}$) are identified by means of their ionization energy loss $\frac{\mathrm{d}E}{\mathrm{d}x}$ in the ALEPH TPC. For all particle types, the inter-jet $\mathcal{R}$ values are seen to increase with increasing momentum (see figure 8). Within given momentum intervals, there is no evidence in the data for a significant mass dependence of the $\mathcal{R}$ values, consistent with the JETSET Monte Carlo predictions.

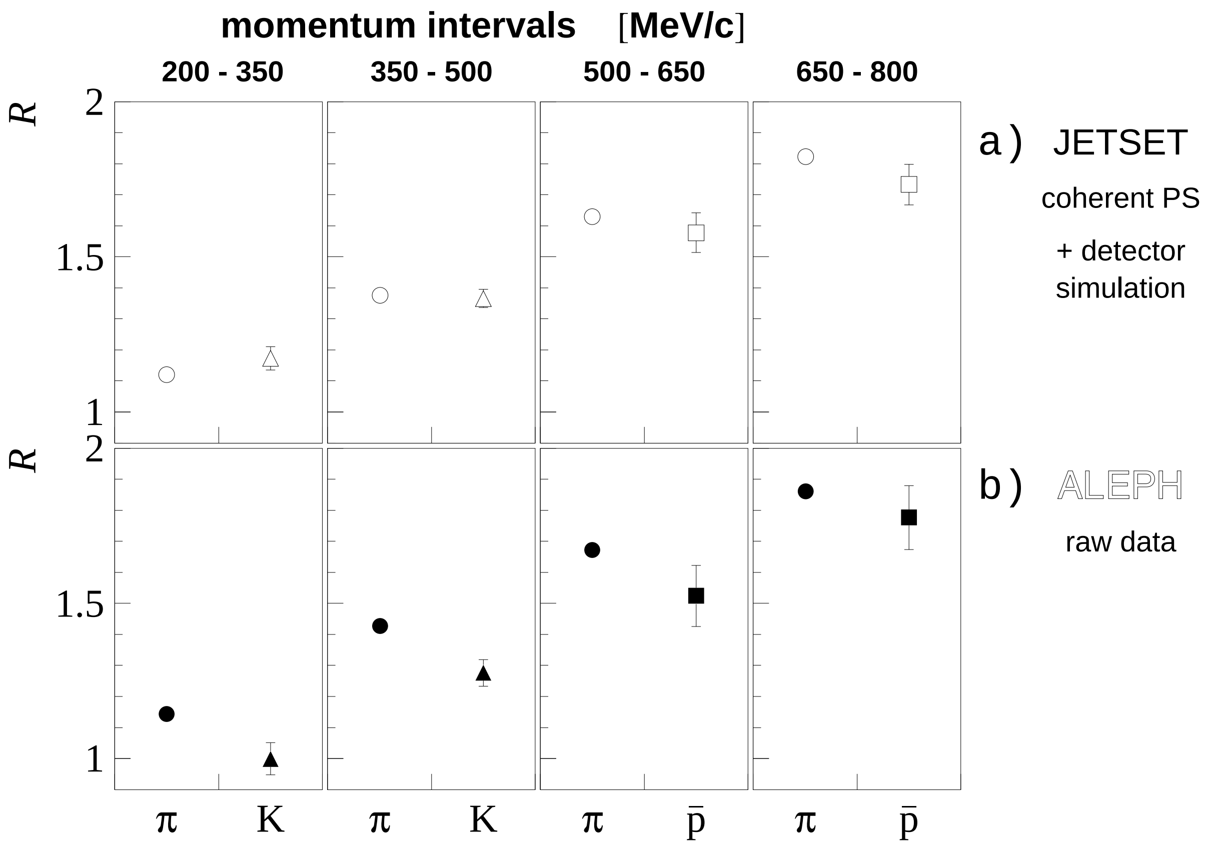

Figure 8: The inter-jet particle flow ratio in momentum intervals as a function of the particle type : a) Monte Carlo prediction and b) ALEPH data. The first two colums show the $\mathcal{R}$-values of pions and kaons and the last two colums compare the $\mathcal{R}$-values of pions and antiprotons. The momentum of the particles considered increases from left to right.

4 Angle shift within jets

In this section a new type of analysis is presented to measure the string effect which makes use of the particle – jet assignments delivered by the cluster algorithm and which is not restricted to interjet regions. The idea is based on the prediction of the Lund string model that low momentum particles in a quark jet are pulled towards the gluon jet. This expected behavior is directly seen in the data and the JETSET Monte Carlo simulation in figure 9 where the average azimuthal particle angle with respect to the jet axis is given as a function of the particle momentum, for the two highest energy jets in 3–jet events from region 3. For jet 1, the $\langle\Delta\phi\rangle$ values are positive

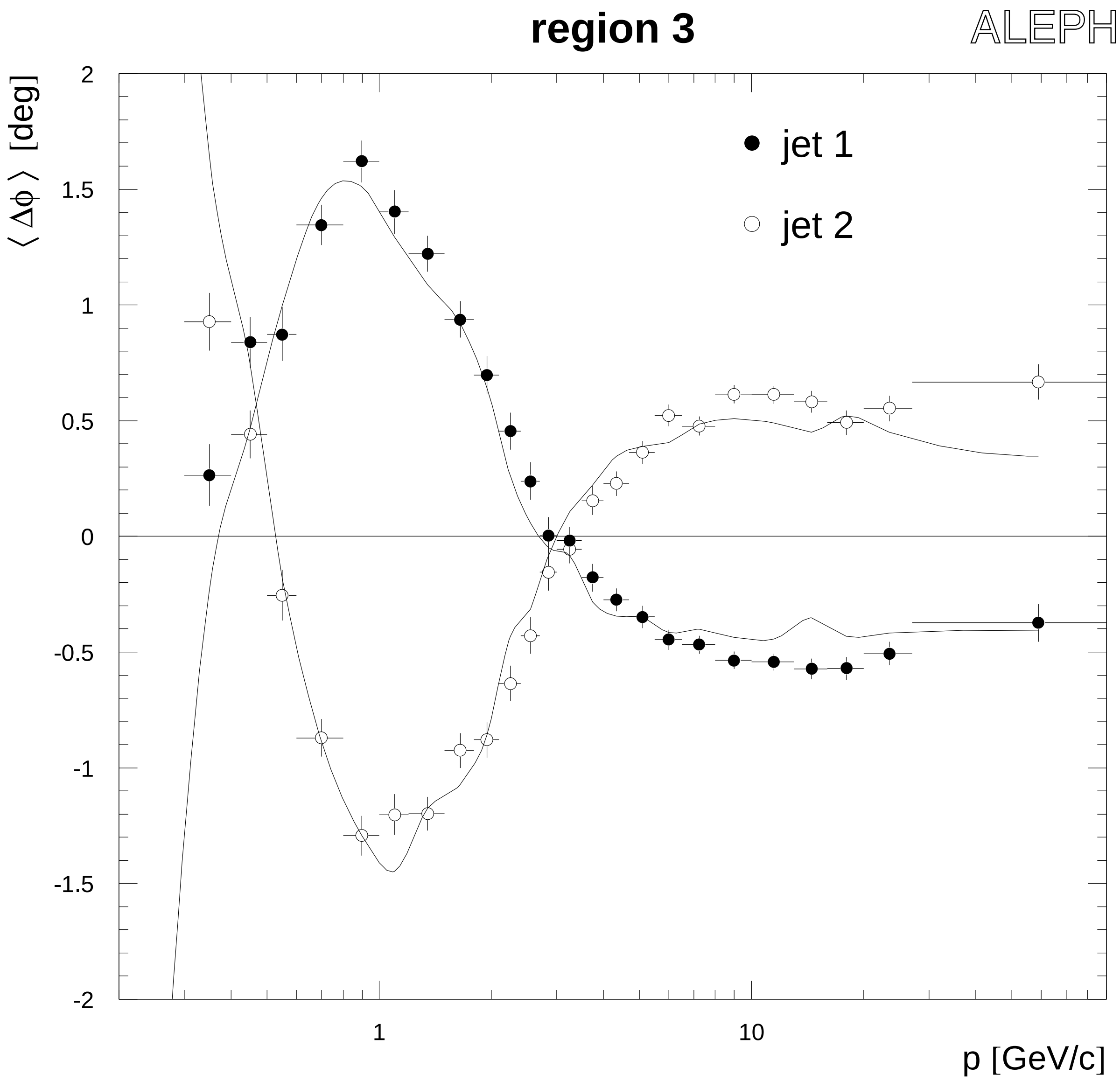

Figure 9: Dependence of the average particle angle with respect to the jet axis as a function of momentum for events from kinematic region 3 and with $y_{cut} = 0.009$. ALEPH 1992 data (uncorrected) are shown as dots. The results from the JETSET Monte Carlo with full detector simulation are superimposed as solid lines.

(*i.e.* towards jet 3) for particle momenta ≈ 1 GeV, change sign at about 3 GeV and stay roughly constant at $\approx -0.5°$ for high momenta. The jet 2 results are almost mirror symmetric. This suggests to define a single variable: the angle difference between high momentum particles and the total jet vector. Several possibilities have been tried and were found to give similar results. QCD model studies show that the leading particle (*i.e.* with the highest momentum in a jet) approximates the underlying hard parton direction on average. The variable studied is

$$\langle \Delta\phi(\mathbf{L1}) \rangle \;=\; \langle \phi(\text{leading particle}) - \Phi(\text{jet}) \rangle,$$

the difference between the highest momentum particle and the total jet vector, which is a measure of the angle shift between parton jet and hadron jet. From simulated events, the resolution of a single $\Delta\phi(\mathbf{L1})$ measurement is found to be dominated by the resolution of the jet axis and has a value of $\approx 1.3°$ for a typical $y_{cut} = 0.01$. The distribution of $\Delta\phi(\mathbf{L1})$ has an rms spread of 4.6° arising mainly from the intrinsic $p_\perp$ in a jet. Nevertheless, the average value of $\approx -0.5°$ can be determined quite accurately. The correction for detector effects is performed by an additive term which is found to be small. The corrected values based on 69 160 events (1992 and 1993 data combined) from region 3 and for $y_{cut} = 0.01$ are :

$$\begin{aligned} \langle \Delta\phi(\mathbf{L1}) \rangle_{jet1} &= -0.57° \pm 0.02(stat) \pm 0.06(syst) \\ \langle \Delta\phi(\mathbf{L1}) \rangle_{jet2} &= +0.62° \pm 0.02(stat) \pm 0.04(syst) \ . \end{aligned}$$

Jet 3 does not discriminate between different QCD models and is therefore ignored. The systematic errors are estimated by varying the experimental cuts and by using different QCD generators to perform the corrections. The numbers given above clearly demonstrate an angle shift effect present in the data.

The analysis has been performed over a large range of y_{cut} values from 0.001 to 0.1. The results for the two highest energy jets are shown in figure 10 for the most sensitive kinematic region **R3**. The average angle shift is seen to vary only slightly and appears to have a maximum at around y_{cut} = 0.006. It should be noted that neighboring data points are strongly correlated due to overlap of the event samples.

The comparison of the data with QCD models in figure 10 leads to conclusions which are similar, though not identical, to those made in the previous section. Concerning the variation with y_{cut}, the predictions of the different shower models are seen to come closer to each other and to the data for smaller y_{cut} values, indicating the decreasing importance of differences in the shower treatment for narrower jets. The main difference to the results from the $\mathcal{R}$ analysis is that the standard JETSET coherent parton shower model predicts a somewhat lower effect than seen in the data at y_{cut} values around 0.01. Including azimuthal interference raises the angle shift in good agreement with the jet 1 data but slightly too much for jet 2. Switching off angular ordering gives a worse description of the data. While the HERWIG generator predicts, like JETSET a too small effect, ARIADNE predicts a much too high effect. In contrast to the previous section, here the JETSET matrix element model is seen to behave differently from the parton shower model. The closed string option as well as independent fragmentation cannot describe the data.

5 Summary

Three–jet events selected from a large sample of Z $\rightarrow$ hadrons events by the $k_\perp$ cluster algorithm have been examined in terms of the color string effect arising from the hard gluon. According to perturbative QCD, the lowest energy jet (= jet 3) is the gluon jet with high probability. Two observables, the inter-jet particle flow $\mathcal{R}$ and the angular shift $\langle \Delta\phi(\mathbf{L1}) \rangle$ between the leading particle and the total jet vector for jets 1 and 2, are measured and compared to QCD model calculations.

The string effect is clearly observed in both analyses. The inter-jet effect is seen to grow with particle momentum. For charged hadrons (π, K and $\overline{\mathrm{p}}$) there is no evidence for a mass dependence of $\mathcal{R}$ at fixed momentum.

QCD event generators based on the leading-log parton shower plus a model to describe hadronization (the string in JETSET and clusters in HERWIG) are in general in rough agreement with the measurements. At values for the jet resolution parameter y_{cut} around 0.01, JETSET agrees well with the $\mathcal{R}$ data but slightly underestimates the angle shift. HERWIG shows a slightly

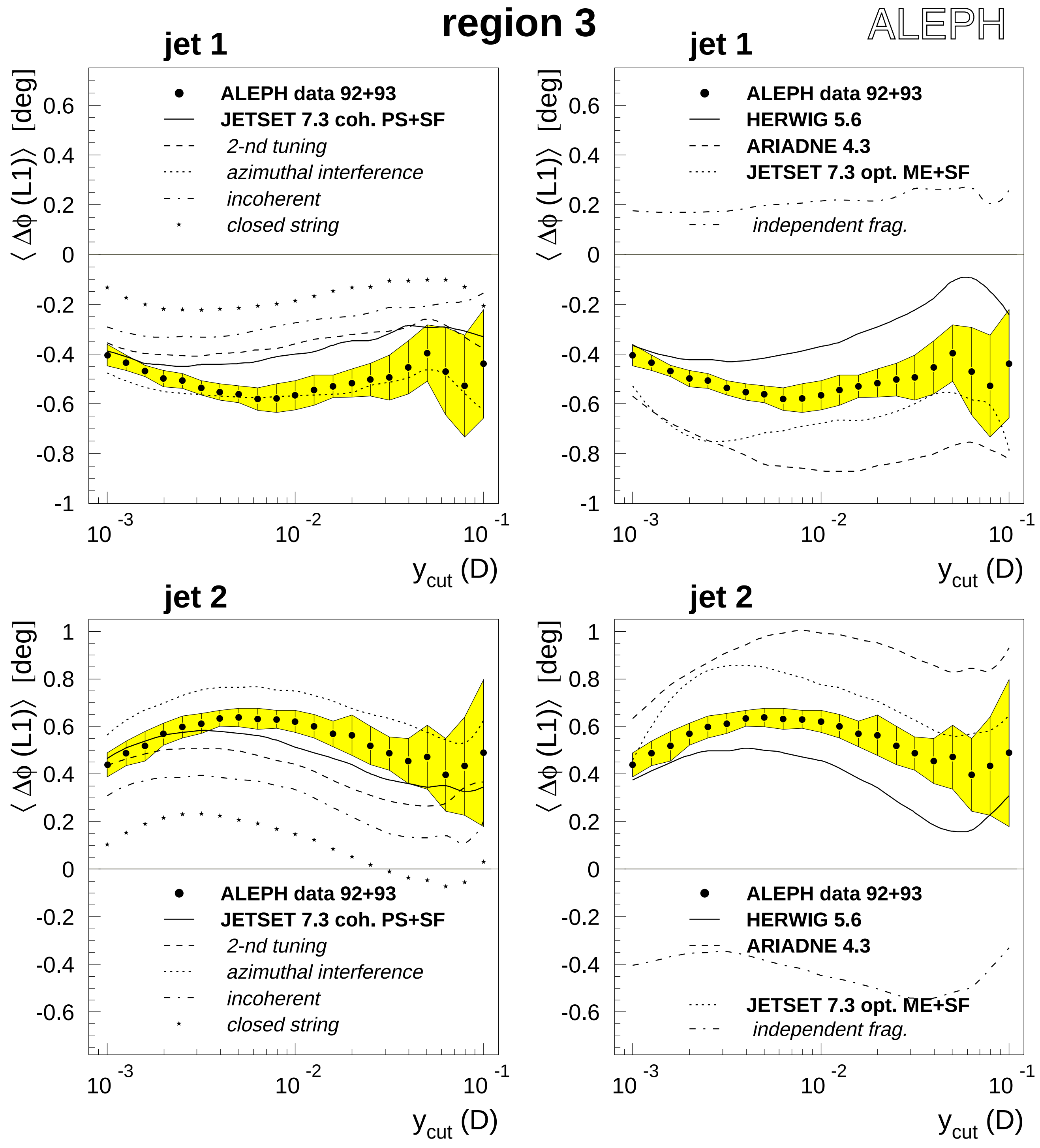

Figure 10: Dependence of the angle shift $\langle\Delta\phi(\mathbf{L1})\rangle$ in jets 1 and 2 on the resolution parameter y_{cut} for events from kinematic region **R3**. The corrected data are shown as dots with error bands giving the combined statistical and systematic error. The predictions of several QCD models are superimposed.

too small effect with both methods. Switching off the angular ordering (= soft gluon coherence) in the shower leads to a worse description. The ARIADNE model which is based on a color dipole formulation of the parton cascade, predicts a too large string effect, while independent jet fragmentation models underestimate it.

Within the context of QCD event generators the string effect is built up by both perturbative (coherence) and non-perturbative contributions. On the perturbative level the most important effect appears to be angular ordering, but also azimuthal interference gives a sizeable contribution. The ARIADNE model is almost able to saturate the experimental results already on parton level. Combined with string fragmentation the effect is overestimated. Non-perturbative contributions to the string effect, even of comparable magnitude, can arise not only in the string fragmentation scheme, but also in the HERWIG cluster model and even in the COJETS independent fragmentation scheme. An alternative independent fragmentation scheme available in the JETSET program does not exhibit the string effect.

Acknowledgements

We would like to thank our colleagues of the CERN accelerator divisions for the excellent performance of the LEP accelerator. Thanks are also due to the many engineering and technical personnel at CERN and at the home institutes for their contributions toward the success of ALEPH. Those of us not from member states wish to thank CERN for its hospitality.

References

[1] JADE Collab., W. Bartel *et al.*, Phys. Lett. **101B** (1981) 129.

[2] JADE Collab., W. Bartel *et al.*, Z. Phys. **C21** (1983) 37.

[3] TPC/2γ Collab., A. Aihara *et al.*, Z. Phys. **C28** (1985) 31.

[4] TASSO Collab., M. Althoff *et al.*, Z. Phys. **C29** (1985) 29.

[5] JADE Collab., W. Bartel *et al.*, Phys. Lett. **134B** (1985) 31;
TPC/2γ Collab., A. Aihara *et al.*, Phys. Rev. Lett. **54** (1985) 270.

[6] OPAL Collab., M. Akrawy *et al.*, Phys. Lett. **261B** (1991) 334.

[7] ALEPH Collab., D. Buskulic *et al.*, Performance of the ALEPH detector at LEP, CERN-PPE/94-170, submitted to Nucl. Instr. Meth. A

[8] Durham Workshop, W.J. Stirling, J. Phys. **G**: Nucl. Part. Phys. **17** (1991) 1567.

[9] ALEPH Collab., D. Buskulic *et al.*, Z. Phys. **C55** (1992) 209.

[10] T. Sjöstrand, Comp. Phys. Comm. **82** (1994) 74.

[11] G. Marchesini, B. R. Webber *et al.*, Comp. Phys. Comm. **67** (1992) 465.

[12] L. Lönnblad, Comp. Phys. Comm. **71** (1992) 15.

[13] R. Odorico, Comp. Phys. Comm. **59** (1990) 527; DFUB 92-6 (1992)